BioGecko

Vol 12 Issue 03 2023
ISSN NO: 2230-5807

Synthesis, characterization and *in vivo* evaluation of mannose anchored stearylamine for hepatocytes targeting of nanocarriers

Raghwendra Waghmode[1],Pritam Chaudhari[2],Vipul Sansare[3]*, Anuya Babar[1], Madhuri Desai[11]Faculty of Pharmacy, Krishna Vishwa Vidyapeeth, Karad, Maharashtra, 415539, India.
[2]Department of Pharmaceutical Chemistry, Govindrao Nikam College of Pharmacy, Sawarde, Chiplun, Maharashtra, 415606, India,
[3]Department of Pharmaceutics, Dnyandeep College of Pharmacy, Boraj, Khed, Maharashtra, 415709, India.

Address for correspondence
Dr. Vipul A. Sansare
Department of Pharmaceutics, Dnyandeep College of Pharmacy, Boraj, Khed, Maharashtra, 415709, India.
vipulsansare@gmail.com,
+91-9322716637

ABSTRACT
Sesamolis a well-recognized antioxidant phytoactive isolated from sesame oil. Benzodioxole group of sesamol has potential to scavenge hydroxyl radical that impart hepatoprotective potential to such phytoactive. Mannose, a water soluble monosaccharide washydrophobized by covalent attachment of stearylaminewith an objective of efficient surface conjugation of mannose in sesamol loaded nanostructured lipid carriers for targeting asialoglycoproteinreceptors on hepatocytes. Mannose anchored stearylamine was synthesized and characterized using sensitive analytical techniques. The synthesized targeting ligand was incorporated sesamol loaded nanostructured lipid carriers and characterizedby photon correlation spectroscopy as well as hemolytic toxicity. Zeta potential measurement was used to confirm surface conjugation of synthesized ligand to drug loaded nanostructured lipid carriers. CCl_4 induced hepatotoxicity in male Wistar ratwas used as experimental animal model to evaluate hepatoprotective potential of formulated drug encapsulated nanostructured lipid carriers. Both mannose conjugated and unconjugated drug loaded nanosystems were evaluatedfor *in vivo* hepatoprotective potential using Liv-52 was used as standard drug. On completion of treatments hepatoprotective potential was assess by measuring serum liver injury markers and oxidative stress parameters in liver post–mitochondrial supernatant. Mannose conjugated nanoformulation showed acceptable particle size and minimum hemolytic toxicity which revealed its suitability for hepatocytes targeting. The mannose conjugated nanostructured lipid carriers revealed significantly better ($p < 0.05$) reduction of serum liver injury markers and proinflammatory cytokine compared to unconjugated one which confirmed hepatocytes targeting potential of synthesized ligand. Thus synthesized mannose anchored stearylamine could be novel targeting ligand having hepatocyte targeting potential.

KEYWORDS: D-mannose; Stearylamine conjugate;Asialoglycoprotein receptors; Sesamol; Antioxidant; Nanostructured lipid carriers; hepatocytes targeting

Introduction

Liver is complex andspecialized organ which regulate numerous biochemical functions like synthesis and metabolismof number of complex molecules.Various liver diseases affect millions of peopleworldwide, which are difficult to treat with conventional drug delivery[1]. World health organization has reported 30 to 50% of liver cirrhosisglobally due to alcohol consumption and more than 300 million cases of chronic

hepatitisinfections in 2020[2]. Numerous drugs have been investigated for treatment of diseases associated with liver however correct drug delivery system need to be find for delivery of drugs.

Majority of conventionally administered drugs are accumulate in liver however the efficient therapeutic effect in diseases like hepatocellular carcinoma, hepatitis, liver cirrhosis and hepatic tuberculosis is not achieved. To overcome limitations associated with conventional drug delivery of phytoactives the novel colloidal carriers like Liposomes[3–6], niosomes [7–9], polymeric nanoparticles (NPs)[10–13], solid lipid nanoparticles (SLNs)[14–17], nanostructured lipid carriers (NLCs)[18–21] and phytosomes [22–25] were widely investigated by many formulation scientists.

These colloidal carriers offer numerous advantages including ease of surface conjugation with targeting ligand for cell specific delivery[26]. Hepatocytes targeting is a challenging concept to the formulation experts because lack of surface receptors expression on these cells. The carbohydrate receptors expressed on hepatic parenchymal cells arecalled as asialoglycoprotein receptor[27]. These receptors specifically recognize carbohydrates like mannose, galactose, fructose and fucose[3]. Thus conjugation of these carbohydrates on surface of drug loaded nanocarriers could be promising strategy for hepatocytes specific delivery of drug. In addition to this, carbohydrates have better potential to bind with receptors expressed on various cell types and can also provide a stealth protection to the colloidal carriers like liposome and NPs[28,29]. Numerous researchers have successfully utilized carbohydrate as targeting ligand for liver targeting of drug encapsulated nanocarriers.

Wu et al. 2009 [30] have attempted to formulate prednisone loaded NPs for liver targeted drug delivery using galactose as a targeting ligand. The *in vivo*studies proved better targeting potential of galactose modified drug loaded NPs compared to conventional NPs. The studies also showed better uptake of galactose decorated drug loaded NPs in liver. This could be due to surface conjugation of NPs with galactose which is responsible for liver specific delivery of NPs. Guo et al. 2014 [31]have utilized galactose as targeting ligand for hepatocytes targeted delivery of doxorubicin. The fabricated drug loaded NPs revealed better uptake of drug in liver ascompared to kidney and heart. Craparo et al. 2014 [32]have successfully proved use of galactose for liver targeted delivery of sorafenib. The galactose modified sorafenib encapsulated micelles showed specific distribution in mice liver on oral administration. Bei et al. 2014[33]have formulated lactose conjugated self-assembled micelles for hepatocytes specific delivery of harmine. Formulated drug loaded micelles exhibited significantly better inhibition of tumor growth in H22 tumor bearing mice. In addition to this fluorescence spectroscopy confirmedbetterliver targeting potential of lactose modified micelles. The major findings of these studies can suggest the use of carbohydrates for efficient liver targeting of drug loaded nanocarriers.

Carbon tetrachloride (CCl_4) induced hepatic injury is thebest suitable animal model of free radical-mediated hepatotoxicity [34]. Metabolism of CCl_4results in formation of trichloromethyl freeradical, CCl3*. The resulted free radicalmediate production of reactive oxygen species through cytochrome P450 oxygenase system. The reactive oxygen species causes lipid peroxidation and lastly hepatocellular damage. CCl3* interacts with cellular molecules like nucleic acid, protein and lipid which eventually leads to lipid metabolism impairment and fatty degeneration i.e. steatosis.Sesamol (SM), 5-hydroxy-1, 3-benzodioxole or3,4-methylenedioxyphenol is a well-known antioxidantphytoactive isolated from sesame oil[35,36]. Benzodioxole group of sesamol has ability scavenge hydroxyl radical that impart hepatoprotective potential to such phytoactive[37].

The aim of the present work was synthesis and characterization of a mannose conjugated stearylamine with potential to target the asialoglycoproteinreceptor of hepatocytes. Mannose and stearylamine was synthesized and characterized by advanced analytical techniques and incorporated into SMloaded NLCs which were evaluated by photon correlation spectroscopy. Hepatoprotective potential of fabricated SM loaded NLCs was assess using CCl_4 induced hepatotoxic animal model. The mannose decorated NLCs showed significantly better hepatoprotection compared to unconjugated NLCs.

Material and methods

Material

Sesamol, D-mannose and stearylamine were purchased from Sigma-Aldrich Co. LLC (St. Louis, USA). Soya lecithin S-100 was kindly gifted by Lipoid (Germany). Dynasan 118® and stearic acid were purchased from Sasol Germany GmbH (Germany). Oleic acid and Tween 20 were purchased from S.D. Fine Chemicals Ltd. (Mumbai, India). Compritol 888 ATO, Precirol 5® and Geleol® werepurchased from Gattefosse, (USA).All other reagents, solvents and chemicals were analytical grade and purchased locally.

Methods

Synthesis of N-octadecyl-mannopyranosylamine

Synthesis was carried out by method as reported by Witoonsaridsilp W et al.[38] with slight modification. Briefly, a 5 mM of stearylamine was dissolved in 15 ml ethanol and heated up to 70°C, after which 5 mM of D-mannose was added with continuous stirring (200 rpm). This solution was stirred for 15 min till mannose was completely dissolved. The solution was cooled to 40°C and diluted with 35ml n-hexane to precipitate NODM. The obtained crystals of NODM then collected by vacuum filtration and purified using dialysis technique. The reaction was monitored with thin layer chromatography. Hexane: ethyl acetate (8:2) was used as mobile phase and spots were detected in presence of UV light.

Characterization of NODM

Fourier-transform infrared spectroscopy (FTIR)

FTIR spectrums of mannose, stearylamine and synthesized NODM were recorded using Jasco FTIR-5300 (Japan) by the KBr disk technique. Briefly all samples (3 mg) were geometrically mixed with KBr (300 mg) separately and resulting mixture compressed into a thin disk in a die at pressure of 10 ton to form thin KBr disk. At last spectrums were recorded.

Proton nuclear magnetic resonance (^{1}H NMR)

^{1}H NMR spectrum of synthesized NODM was recorded on a Bruker Avance II400 NMR spectrometer at 400 MHz. ^{1}H NMR was recorded using$CDCl_3$ as solvent.

Fabrication of conventional and mannose decorated SM loaded NLCs

Conventional and mannose conjugated SM encapsulated NLCs were formulated by melt homogenization ultrasonication technique. In practice SMwith or without NODM (10% w/w of total lipid) were dissolved in molten stearic acid: oleic acid (8:2)mixture and soya lecithin S-100 was transferred in resulting melted lipid. An aqueous stabilizer solution containing 10 ml of distilled water and Tween 20 was injected using syringe (24 gauge) into molten lipid mass and stirred at 4000 rpm for 10 minutes at 70°C using overhead stirrer (Remi, India).The obtained pre emulsion was subjected to probe sonication (VCX500, Sonics and materials, U.S.A.) at 20% amplitude for 10 minutes and cooled to room temperature. The resulting NLC dispersion was subjected to homogenization using high pressure homogenizer (Stansted, UK) at 10,000 psi for 3 cycles.

Characterization of SM loaded NLCs

Dynamic light scattering

Particle size distribution of both mannose conjugated and unconjugated SM loaded NLCs were studied using photon correlationspectroscopy (Zetasizer Nano ZS, Malvern instruments, Worcestershire, UK). NLCs dispersions were diluted with double distilled water and subject to particle size measurement at 24 ^{0}C[39].

Assessment of entrapment efficiency of SM

The percentage entrapment efficiency of SM in the SM loaded NLC dispersions was determined using the indirect method. The SM loaded NLC dispersions were subjected to ultra-centrifugation at 80,000 rpm for 1h at 4°C using Optima Max XP ultracentrifuge (Beckman Coulter, U.S.A.) to separate the unentrapped SM. Supernatant was diluted and analyzed by UV spectrophotometry at λmax of 294 nm using methanol AR as blank for quantification of unentrapped or free SM. Percentage entrapment efficiency was calculated by using equation.

$$\text{Percent entrapment efficiency} = \frac{\text{WL} - \text{WF}}{\text{WL}} \times 100$$

Where, WL is quantity of SM added in dispersion and WF is amount of SM unentrapped.

Animal model and experimental protocol

Male Wistar rats weighing 150 to 200 gm were used as test animals to evaluate liver targeting potential of synthesized ligand. The animal study protocolwas approved bythe Institutional Animals Ethical Committee of Indira Institute of Pharmacy (Approval number: IIP/IAEC/08/2019-20). All animals were purchased from Global bioresearch solution Pvt. Ltd, Shirwal, India.

Rats were housedcages and fed standard diet.Rats were randomly divided into five groups,each having 6 rats. Group I was marked as vehicle control (VC) group and received 1 ml/kg BW olive oil. Group II serve as positive control (PC) and received standard hepatotoxic drug CCl_4. Group III was marked as standard group and received Liv-52 at the dose of 1 ml/kg BW[40]. Group IV animals were treated with mannosylated SM NLCs at the dose of 8 mg/kg BW. Group V animals were treated with conventional SM NLCs at the dose of 8 mg/kg BW.

Hepaticinjury to the 24 experimental animals was induced by oral administration of 4 ml/kgBW CCl_4 (dispersed with an equal volume of olive oil) for 10 days.In VC group 1 ml/kg BW of olive oil was administeredfor 10 days (no hepatic injury as well as treatment in the case of VC group).In standard group three days afterfinal dose of CCl_4, Liv-52 was administeredat a dose of 1ml/kg BW daily for fourweeks.In group IV threedays after last dose of CCl_4 as in thestandard group, mannosylated SM NLCs were administered at adose of 8 mg/kg BW daily for four weeks.In group V three days after last dose of CCl_4 as in the standard group, conventional SM NLCs were administered at adose of 8 mg/kg BW daily for four weeks[41].

At the end of treatment schedule, rats were anesthetized using ether and blood sampling was carried out through retro-orbital plexus. Serum from blood samples was isolated by centrifuging at 4000 rpm for 20 minat 4°C and stored at −20°C for estimation of serum liver injury markers. At the end of treatment protocol all animals were sacrificed by cervical dislocation toharvest theirliver for estimation of oxidative stress parameters. In the PC groupanimals were sacrificed three days post final dose ofCCl_4 i.e. on 13th day and all the other animals were sacrificed on the 42th day, i.e. a day after the final treatment schedule. After harvesting liver was homogenized with 10% (w/v) coldphosphate –buffered saline (PBS pH 7.4).To estimate oxidative stress parameters the liver post –mitochondrial supernatant (PMS) was used. PMS was preparedby centrifugation of rat liver homogenates in thechilled phosphate buffer, pH 7.4 for 20 minat 4°C.

Estimation of Serum Liver Injury Markers

Estimation of serum liver injury markers such as ALT, AST is very important operation to measure hepatoprotective efficacy of SM NLCs and liver targeting efficiency of synthesized ligand.

Serum liver injury markers like ALT, AST were estimated using diagnostickits (Reckon diagnostic, India). The manufacturer protocol was used to perform the assays.

Estimation of antioxidant parameters

The oxidative stress parameters like LPO, SOD and GSH were estimated in liverPMS.

Estimation of LPO

The method of Wills was used for quantitative measurement of LPO in liver PMS [42]. The malondialdehyde(MDA) level, a measure of LPO, was measured asliver thiobarbituric acid reactive species. The LPO level in experimental animalswere expressed as nanomoles of MDA per milligram ofprotein, using the molar extinction coefficient of thechromophore as $1.56 \times 10^5\ M^{-1}\ cm^{-1}$.

Measurement of SOD

The method reported byKono et al. [43] was used for measurement of SOD activity in liver PMS. SOD activity was represented in terms ofunits of SOD per milligram of protein (SOD units/mg Pr).

Estimation of GSH levels

The GSH estimation procedure reported by of Jollow et al. [44] was used for estimation of GSH.The GSH level was measured and expressed as nmoles of GSH per µg ofprotein (nmoles of GSH/µg Pr).

Estimation of pro-inflammatory cytokine, TNF-α

An ELISA kit (RayBiotech, Inc) was used for measurement of TNF-α levels in liver homogenates. The assay was performedaccording to the manufacturer guidelines.

Hemolytic toxicity study

Hemolytic study was performed as per earlier reported method with slight modification[45]. Briefly whole human blood wascollected with EDTA in blood collecting vials (HiMedia, India)and centrifuged at 7000 rpm for 10 minutes. The RBCs werecollected and resuspended in normal saline. In 2 ml RBCssuspension, 4ml distilled water was added, which was considered to produce 100 % hemolysis. Similarly 4 ml of normal saline was added in 2ml RBCs suspension assumed to produce no hemolysis. 2 ml of mannosylated SM NLCs and conventional SM NLCs were added separately in 2 ml RBCs suspension and incubated for 2 hours. At the end of 2 hoursthe formulations were centrifuged at 7000 rpm for 10 minutes andsupernatants were collected. The absorbance of supernatantmeasured spectrometrically and % hemolysis was calculated,using following equation. All experiment were performed intriplicates and values expressed graphically as mean± SD.

$$\%\ \text{Hemolysis} = \frac{\text{Abs} - \text{Abs}\ 50}{\text{Abs}\ 100 - \text{Abs}\ 50} \times 100$$

Where Abs is the absorbance for the test sample. Ab50 is theabsorbance of sample with 0% hemolysis. Ab100 is the absorbance sample with100% hemolysis.

Statistical Analysis

All animal experimental data wasanalyzed through one way analysis of variance (ANOVA),followed by the Tukey test for comparison of means varioustreatments. Differences between the means were consideredstatistically significant at $p < 0.05$.All experimental data expressed as mean ± standard deviation (SD).

Results and discussion

Synthesis of NODM

The reaction of unprotected hydroxyl group of monosaccharides with long hydrocarbon chain amines in alcoholic medium has reported in scientific literature [46]. In present reaction, unprotected hydroxyl group ofmannose reacted with amine group of stearylamine, resulted in formation of secondary amine bond between them. The obtained NODM was pale yellow crystals with the yield in range of 78.61 to 84.13%.The physical characteristics like colour as well as solubility of both mannose and stearylamine were examined to preliminarily confirm product formation from resulting reaction. The examined physical characteristics are highlighted in Table 1. D-mannose was white, water soluble powder whereas synthesized NODM was pale yellow crystals with solubility in organic solvent. There was change in the solubility pattern of mannose and NODM confirming formation of new reaction product.

Fourier-transform infrared spectroscopy (FTIR)

FTIR spectrum of D-Mannose, stearylamine and synthesized NODM were recorded and shown in Figure 1. In spectrum of D-Mannose, broad peak at 3398 $cm^{-1}$and intense peak at 2926 cm^{-1}indicate the presence of –OH stretching and –CH2 stretching vibrations. Vibrational signals at 1064 and 1638 cm^{-1}indicate C=O stretching of either alcohol or aldehyde groups in mannose. In the spectrum of stearylamine, sharp lower intensity peak at 3331 cm^{-1} indicate –NH2 stretching of primary amine group of stearylamine. Vibrational signals at 2917 and 2849 cm^{-1}indicate –CH2 stretching of long alkyl chain. These two peaks were found to be more intense than that of mannose due to presence of long alkyl chain in stearylamine. Vibrational peaks at 1606 and 1471 cm^{-1}indicate presence of –NH2 and –CH2 bending. Spectrum of NODM showed lower intensity peak at 3383 cm^{-1}. This is due to combination of –NH2 stretching of stearylamine and –OH stretching of mannose. Peak at 1606 cm^{-1}observed in stearylamine appear at lower intensity in NODM, indicating the conversion of primary amine (stearylamine) to secondary amine (NODM). Reduced intensity of peaks at 1606 $cm^{-1}$and 3383 cm^{-1}indicates the secondary amine linkage between mannose and stearylamine.

^{1}H NMR

Proton NMR spectrum of synthesized NODM is represented in Figure 2.In proton NMR spectrum, presence of lower intensity -NH proton signal at 2.7 ppm indicates the secondary amine linkage between mannose and stearylamine which confirms the conjugation.

Characterization of SM loaded NLCs

NODM was incorporated into the NLCs by a melt homogenization ultrasonication technique. NLCs with and without NODM werecharacterized for their size and entrapment efficiency. The conventional and mannosylated SM NLCs revealed particle size of 142.8 and 145.1 nmrespectively asshown in Figure 3 and 4.Particle size of nanocarrier governs their uptake in hepatic parenchymal cells[47,48]. The numerous scientific experts have reported thatnanocarriers with particle size less than 200 nm can efficiently engulf byhepatic parenchymal cells and generate significant biological effect. Both drug loaded NLCs revealed particle size less than 200 nm which confirm its suitability for hepatic targeted drug delivery. The Entrapment efficiency of SM in conventional and mannosylated NLCs was found to be 71.23 and 69.62 %.

NODM SM NLCsrevealed lower zeta potential than conventionalSM NLCsas represented in Table 2. The mannose conjugation on the surface of NLCs was confirmed by the zeta potential study. The decrease in the zeta potential value ofSM loaded NLCs with increase concentration of NODM in NLCs from zero to 10% w/w of totallipids were major findings of present study. The reduction in the zeta potential, from -15.28 to -39.86 mV for the conventional SM NLCs and the NODM conjugated SM NLCs at 10% NODM concentration respectively,could be attributed to the presence of mannose on the surface of NLCs as they contribute negative charge due to presence of ionizable hydroxy (OH^-) group.

The decrease zeta potential of SM loaded NLCs with increase NODM concentration confirmed presence of NODM on the surface of the NLCsas desired for the hepatocytes targeted delivery of SM. Thus zeta potential experiment was successfully utilized to validate incorporation of NODM on SM NLCs surface.

Serum liver injury markers

AST and ALT enzymes are release in plasma due to damage of structural integrity ofhepatic cells. Elevation of AST and ALT levels due to administration of CCl_4in experimental animals confirmed hepatic cellular damage[49].CCl_4administration in experimental animals resulted in 2368.06% elevation in ALT level compared to group I (VC). The elevated level of serum liver injury marker like ALT was sign of hepatotoxicity induction in rats. The four weeks treatment with conventional SM NLCs and mannosylated SM NLCs resulted significant reduction in elevated ALT levels by 51.48 ± 3.61% and 60.41 ± 3.46% respectively as highlighted in Table 3. Liv-52 (Group III) administration in hepatotoxic rats resulted 45.75 ± 2.78% reduction in ALT level. The formulated mannose anchored SM NLCs based dispersion was quite successful in significant reduction ($p < 0.05$) of elevated ALT level in experimental animals compared to conventional SM NLCs and Liv-52. This could be attributed due to hepatocytes targeting potential of synthesized NODM.

In similar way, AST level was elevated by 980.73% due to administration of CCl_4 compared to group I (VC). The conventional SM NLCs reduced elevated AST level by 74.62 ± 3.73%. However mannosylated SM NLCs revealed significantly better ($p < 0.05$) reduction of elevated AST compared to conventional SM NLCs. Thus hypothesis of hepatocyte targeting potential of NODM was confirmed on the basis of significantly better results with mannosylated SM NLCs.

Sesamol has reported to have anti-MMP-9 (matrix metallopeptidase 9) potential[50]. MMP-9 enzyme is involved in necrosis of hepatocytes results in release of ALT and AST from liver[51]. Sesamol inhibits MMP-9 activity and protectsliver against tissue necrosis, by reduction of ALT as well as AST.

Antioxidant parameters

LPO

LPO measured as MDA content in liver PMS.CCl_4 administration resulted in elevation in MDA level by 443.39%. The four week treatment with mannosylated SM NLCs and conventional SM NLCs resulted in reduction in MDA content by 50.31 ±2.31% and 63.48 ± 3.47% respectively. The standard drug Liv-52

reduce elevated MDA content by 50.74 ± 3.57% on four week treatment. The SM loaded NLCs showed significantly better results ($p < 0.05$) compared to standard drug. (Figure 5).

SOD

The positive control CCl_4 group revealed significantly low ($p < 0.05$) SOD level (0.463 ± 0.119 SOD units/ mg Pr) compared to VC group. Treatment with standard drug Liv-52 for four weeks showed 3 times increase (1.5435 SOD units/ mg Pr) in SOD level. The mannosylated SM NLCs treatment resulted in 6 times increase (3.0225 SOD units/ mg Pr) in SOD level whereas conventional SM NLCs treatment showed 4 times increase in SOD level (2.1271SOD units/ mg Pr)(Figure 6). The mannosylated SM NLCs revealed significantly better ($p < 0.05$) results than conventional SM NLCs with respect to elevation of reduced SOD level. This could be attributed due to better uptake of mannose anchored SM NLCs in hepatocytes than that of conventional SM NLCs.

GSH

The total GSH level in PC group was significantly low($p < 0.05$) by CCl_4 administration as compared to VC group. The mannosylated SM NLCs successfully increased total GSH level by 7.87 times on four weeks treatment. The conventional SM NLCs showed comparable results with increase in total GSH level by 6.23 times however it was found to be less effective compare to mannosylated SM NLCs(Figure 7). The Tukey test showed significant difference ($p < 0.05$) between results showed by mannosylated SM NLCs and conventional SM NLCs.

Proinflammatory cytokine TNF-α

The administration of CCl_4 resulted in significant elevation of proinflammatory cytokineTNF-α level (608.73 ± 10.62 TNF Pg/ml) in PC group. The elevation of TNF-α level was indication of hepatic injury induction. The four weeks treatment with mannosylated SM NLCs significantly reduced ($p < 0.05$) the increased levels of TNF-α (197.15 ± 4.68 TNF Pg/ml) compared to conventional SM NLCs (216.49 ± 4.02 TNF Pg/ml)(Figure 8). The Liv-52 treatment showed vast reduction ofTNF-α level (152.61 ± 4.95 TNF Pg/ml). The results obtained with Liv-52 were far better than both SM loaded NLCs.

Hemolytic toxicity study

Free SM showed hemolytic toxicity up to36.064 ± 1.29%. The SM NLCs and Mannosylated SM NLCs exhibited hemolytic toxicity up to20.192 ± 0.971 % and 7.351 ± 1.146 % respectively (Figure 9). The reduction in hemolytic toxicity ofdrug loaded NLCs in comparison to free SMcould be due to the encapsulation of SM in a biocompatiblelipid matrix.Mannoseconjugation to the NLCs surface significantly lowered hemolytictoxicity due to inhibition of interaction of the charge lipid groupand RBCs related with nonconjugated NLCs.

Conclusion

In current investigation, an attempt has been made to synthesize novel hepatocytes targeting ligand i.e. NODM for efficient delivery of sesamol encapsulated NLCs. FTIR and ^1H NMR techniques confirmed correctness of adopted synthetic procedure. Melt homogenization ultrasonication technique was found to be effective method for fabrication of SM loaded NLCs. The selected method was found to be suitable for generation of NLCs with better particle size and SM entrapment efficiency. The particle diameter of NLCs less than 200 nm confirmed its suitability for hepatocyte targeted drug delivery. *In vivo* hepatoprotective potential studied in CCl_4 induced liver injury animal model confirmed hepatocytes targeting potential of synthesized NODM by effectively reducing serum liver injury markers and proinflammatory cytokines compared to conventional NLCs. Thus synthesized mannose anchored stearylamine i.e. NODM could be viable alternative for hepatocyte targeting of nanomedicines.

Acknowledgments

Authors would like to say thanks to Departmentof Pharmaceutics, Bombay College of Pharmacy (Mumbai, India) and Departmentof Pharmacology, Indira Institute of Pharmacy (Sadavali, India) for excellent technical support.

Disclosure statement

Author declare no conflicts of interest associated with thispublication and there has been no significant financial support for this work that could haveinfluenced its possible outcomes.

References

[1] Bartneck M, Warzecha KT, Tacke F. Therapeutic targeting of liver inflammation and fibrosis by nanomedicine. Hepatobiliary Surg Nutr. 2014;3:364–376.
[2] Vasanthkumar T, Hanumanthappa M, Bt P, et al. Hepatoprotective Effect of Curcumin and Capsaicin against Lipopolysaccharide Induced Liver Damage in Mice. Pharmacogn J. 2017;9:947–951.
[3] Shah SM, Pathak PO, Jain AS, et al. Synthesis , characterization , and in vitro evaluation of palmitoylated arabinogalactan with potential for liver targeting. Carbohydr Res. 2013;367:41–47.
[4] Shariare MH, Rahman M, Lubna SR, et al. Liposomal drug delivery of Aphanamixis polystachya leaf extracts and its neurobehavioral activity in mice model. Sci Rep. 2020;10:6938.
[5] Moghimipour E, Aghel N, Mahmoudabadi AZ, et al. Preparation and Characterization of Liposomes Containing Essential Oil of Eucalyptus camaldulensis Leaf. Jundishapur J Nat Pharm Prod. 2012;7:117–122.
[6] Tian J, Wang L, Wang L, et al. A wogonin-loaded glycyrrhetinic acid-modified liposome for hepatic targeting with anti-tumor effects. Drug Deliv. 2014;21:553–559.
[7] Hao Y, Zhao F, Li N, et al. Studies on a high encapsulation of colchicine by a niosome system. Int J Pharm. 2002;244:73–80.
[8] Kalaiselvi A, Gnanaleela J, Jeno A, et al. Chemical composition of clove bud oil and development of clove bud oil loaded niosomes against three larvae species. Int Biodeterior Biodegrad. 2019;137:102–108.
[9] Trinh LH, Takzare A, Ghafoor DD, et al. Trachyspermum copticum essential oil incorporated niosome for cancer treatment. J Drug Deliv Sci Technol. 2019;52:818–824.
[10] Raposo D, Costa R, Petrova KT, et al. Development of Novel Galactosylated PLGA Nanoparticles for Hepatocyte Targeting Using Molecular Modelling. Polymers (Basel). 2020;12:1–18.
[11] Guhagarkar SA, Shah D, Patel MD, et al. Polyethylene Sebacate-Silymarin Nanoparticles with Enhanced Hepatoprotective Activity. J Nanosci Nanotechnol. 2015;15:4090–4093.
[12] Yen F, Wu T, Lin L, et al. Naringenin-Loaded Nanoparticles Improve the Physicochemical Properties and the Hepatoprotective Effects of Naringenin in Orally-Administered Rats with CCl 4 -Induced Acute Liver Failure. Pharm Res. 2009;26:893–902.
[13] Que X, Su J, Guo P, et al. Study on preparation , characterization and multidrug resistance reversal of red blood cell membrane-camouflaged tetrandrine-loaded PLGA nanoparticles. Drug Deliv. 2019;26:199–207.
[14] Kakkar V, Kaur IP. Preparation, characterization and scale-up of sesamol loaded solid lipid nanoparticles. Nanotechnol Dev. 2012;2:40–45.
[15] Prathyusha M, Manjunath K, Tippanna S, et al. Bixin loaded solid lipid nanoparticles for enhanced hepatoprotection – Preparation , characterisation and in vivo evaluation. Int J Pharm. 2014;473:485–492.
[16] Mei Z, Chen H, Weng T, et al. Solid lipid nanoparticle and microemulsion for topical delivery of triptolide. Eur J Pharm Biopharm. 2003;56:189–196.
[17] Liu Z, Okeke CI, Zhang L, et al. Mixed Polyethylene Glycol-Modified Breviscapine-Loaded Solid Lipid Nanoparticles for Improved Brain Bioavailability : Preparation , Characterization , and In Vivo Cerebral Microdialys ... Research Article Mixed Polyethylene Glycol-Modified Breviscapine-Lo. AAPS PharmSciTech. 2014;15:483–496.
[18] Bonferoni MC, Rossi S, Cornaglia AI, et al. Essential oil-loaded lipid nanoparticles for wound healing. Int J Nanomedicine. 2018;13:175–186.
[19] Nahr FK, Ghanbarzadeh B, Kafil HS, et al. The colloidal and release properties of cardamom oil encapsulated nanostructured lipid carrier. J Dispers Sci Technol. 2019;42.

[20] Vieira R, Severino P, Nalone LA, et al. Sucupira Oil-Loaded Nanostructured Lipid Carriers (NLC): Lipid Screening, Factorial Design, Release Profile, and Cytotoxicity. Molecules. 2020;25:685.
[21] Carbone C, Caddeo C, Grimaudo MA, et al. Ferulic Acid-NLC with Lavandula Essential Oil : A Possible Strategy for Wound-Healing ? Nanomaterials. 2020;10:898.
[22] Tung BT, Hai NT, Son PK. Hepatoprotective effect of Phytosome Curcumin against paracetamol-induced liver toxicity in mice. Brazilian J Pharm Sci. 2011;53:1–13.
[23] Maiti K, Mukherjee K, Gantait A, et al. Curcumin – phospholipid complex : Preparation , therapeutic evaluation and pharmacokinetic study in rats. Int J Pharm. 2007;330:155–163.
[24] Maiti K, Mukherjee K, Gantait A, et al. Enhanced therapeutic potential of naringenin – phospholipid complex in rats. J Pharm Pharmcology. 2006;58:1227–1233.
[25] Panda VS, Ã SRN. Cardioprotective activity of Ginkgo biloba Phytosomes in isoproterenol-induced myocardial necrosis in rats : A biochemical and histoarchitectural evaluation. Exp Toxicol Pathol. 2008;60:397–404.
[26] Sansare V, Warrier D, Shinde U. Cellular trafficking of nanocarriers in alveolar macrophages for effective management of pulmonary tuberculosis. J Tuberc. 2020;3:1016.
[27] Pranatharthiharan S, Patel MD, Malshe VC, et al. Asialoglycoprotein receptor targeted delivery of doxorubicin nanoparticles for hepatocellular carcinoma. Drug Deliv. 2017;24:20–29.
[28] Irache JM, Salman HH, Gamazo C, et al. Mannose-targeted systems for the delivery of therapeutics. Expert Opin. 2008;5:703–724.
[29] Jain K, Kesharwani P, Gupta U, et al. A review of glycosylated carriers for drug delivery. Biomaterials. 2012;33:4166–4186.
[30] D-Q W, B L, C C. Galactosylated fluorescent labeled micelles as a liver targeting drug carrier. Biomaterials. 2009;30:1363–1371.
[31] Guo H, Zhang D, Li T. In vitro and in vivo study of gal-os self-assembled nanoparticles for liver-targeting delivery of doxorubicin. J Pharm Sci. 2014;103:987–993.
[32] Craparo E, Sardo C, Serio R. Galactosylated polymeric carriers for liver targeting of sorafenib. Int J Pharm. 2014;466:172–180.
[33] Bei Y, Yuan Z, Zhang L. Novel self-assembled micelles based on palmitoyl-trimethyl-chitosan for efficient delivery of harmine to liver cancer. Exp Opin Drug Deliv. 2014;11:843–854.
[34] Rechnagel R, EAJ G. Carbon tetrachloride hepatotoxicity: an example of lethal cleavage. CRC Crit Rev Toxicol. 1973;2:263–297.
[35] Hemalatha G, Pugalendi K, Saravanan R. Modulatory effect of sesamol on DOCA-salt-induced oxidative stress in uninephrectomized hypertensive rats. Mol Cell Biochem. 2013;379:255–265.
[36] Suja K, Jayalekshmy A, Arumughan C. Free radical scavenging behavior of antioxidant compounds of sesame (Sesamum indicum L.) in DPPH (*) system. J Agric Food Chem. 2004;52:912–915.
[37] Chennuru A, Saleem M. Antioxidant, Lipid Lowering, and Membrane Stabilization Effect of Sesamol against Doxorubicin-Induced Cardiomyopathy in Experimental Rats. BioMed Res Int. 2013;934239.
[38] Witoonsaridsilp W, Paeratakul O, Panyarachun B, et al. Development of Mannosylated Liposomes Using Synthesized N -Octadecyl- D - Mannopyranosylamine to Enhance Gastrointestinal Permeability for Protein Delivery. AAPS Pharm Sci Tech. 2012;13:699–706.
[39] Sansare V, Patel N, Patankar N. Design, optimization and characterization of lamivudine loaded solid lipid nanoparticles for targeted delivery to brain. Int Res J Pharm. 2019;10:143–148.
[40] Mayuren C, Reddy VV, Priya SV. Protective effect of Livactine against CCl 4 and paracetamol induced hepatotoxicity in adult Wistar rats. N Am J Med Sci. 2010;2:491–495.
[41] Singh N, Khullar N, Kakkar V, et al. Sesamol loaded solid lipid nanoparticles : a promising intervention for control of carbon tetrachloride induced hepatotoxicity. BMC Complement Altern

Med. 2015;15:142.
[42] Wills E. Mechanisms of lipid peroxide formation in animal tissue. Biochem J. 1966;99:667–676.
[43] Kono Y. Generation of superoxide radical during autooxidation of hydroxylamine and an assay for superoxide dismutase. Arch Biochem Biophys. 1978;186:189–195.
[44] Jollow D, Mitchell L, Zampaglione N, et al. Bromobenzene induced liver necrosis: protective role of glutathione and evidence for 3,4-bromobenzenoxide as the hepatotoxic intermediate. Pharmacology. 1974;11:151–169.
[45] Papazisis K, Geromichalos G, Dimitriadis K, et al. Optimization of the sulforhodamine B colorimetric assay. J Immunol Methods. 1997;208:151–158.
[46] Lockhoff O, Stadler P. Syntheses of glycosylamides as glycolipid analogs. Carbohydr Res. 1998;314:13–24.
[47] Liang H, Yang T, Huang C, et al. Preparation of nanoparticles composed of poly(gamma-glutamic acid)-poly (lactide) block copolymers and evaluation of their uptake by HepG2 cells. J Control Release. 2005;105:213–225.
[48] Hashida M, Takemura S, Nishikawa M, et al. Targeted delivery of plasmid DNA complexed with galactosylated poly(L-lysine). J Control Release. 1998;53:301–310.
[49] Sallie R, Tredger J, Williams R. Drugs and the liver part 1: testing liver function. Biopharm Drug Dispos. 1991;12:251–259.
[50] Kumagai Y, Lin L, Schmitz D, et al. Hydroxyl radical mediated demethylenation of (methylenedioxy) phenyl compounds. Chem Res Toxicol. 1991;4:330–334.
[51] Ohashi N, Hori T, Chen F, et al. Matrix metalloproteinase-9 contributes to parenchymal hemorrhage and necrosis in the remnant liver after extended hepatectomy in mice. World J Gastroenterol. 2012;18:2320–2333.

Table 1. Physical characteristics of mannose and NODM.

Characteristics	**Mannose**	**NODM**
Colour	White	Pale yellow
Solubility	Aqueous solvent	Organic solvent

Table 2. Zeta potentials of NODM SM NLCs (n=3).

Formulation	**Zeta potential (mV)**
Conventional SM NLCs	-15.28 ± 0.71
NODM SM NLCs (1%)	-21.43 ± 0.53
NODM SM NLCs (5%)	-30.71 ± 0.37
NODM SM NLCs (10%)	-39.86 ± 0.47

Table 3. % inhibition in ALT and AST levels in treatment groups with respect to CCl_4 group (n=6).

Group	**% Inhibition of ALT versus CCl_4 group**	**% Inhibition of AST versus CCl_4 group**
Group III	45.75 ± 2.78	73.45 ± 3.51
Group IV	60.41 ± 3.46	79.82 ± 2.81
Group V	51.48 ± 3.61	74.62 ± 3.73

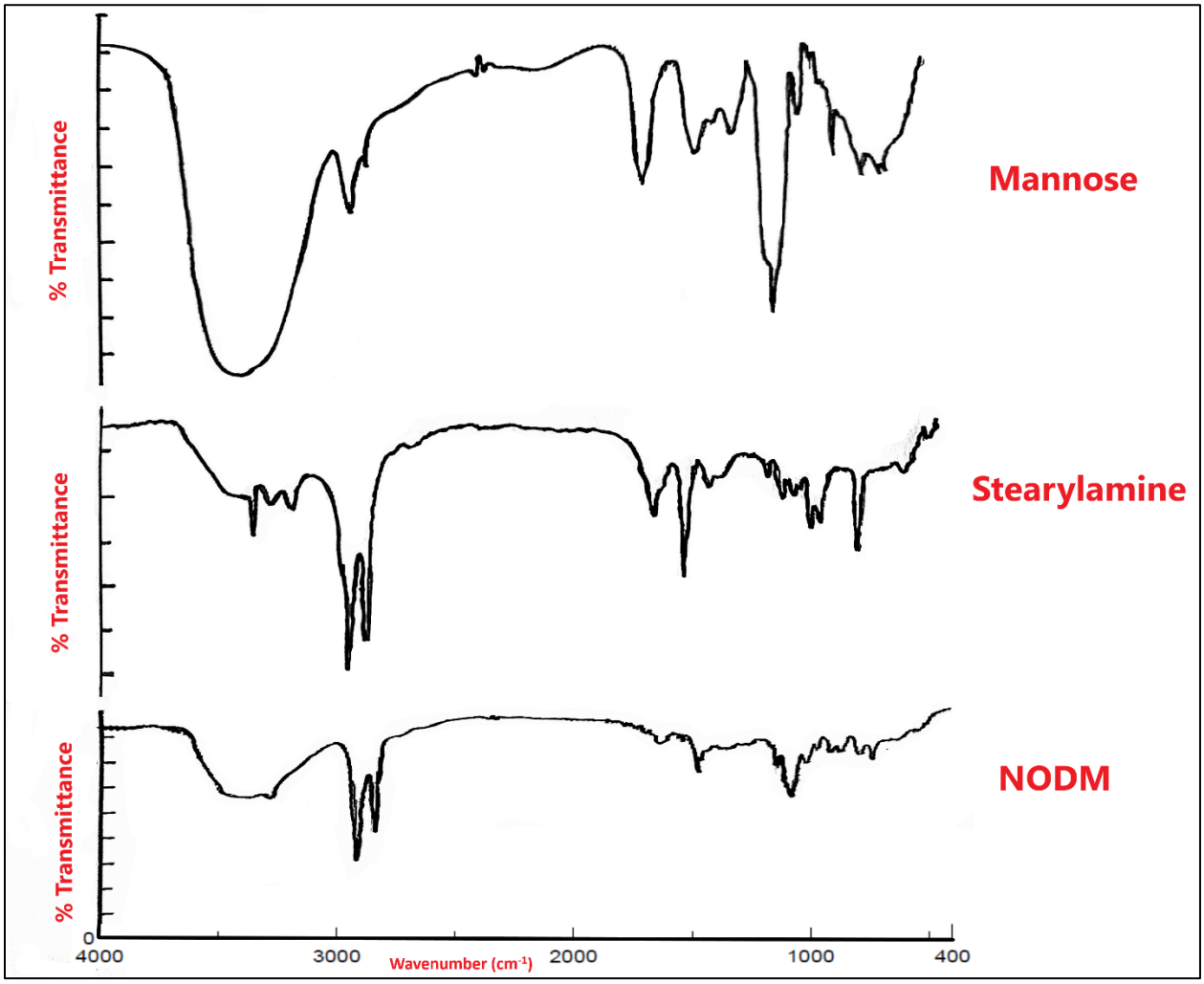

Figure 1. FTIR spectra of mannose, stearylamine and synthesized NODM.

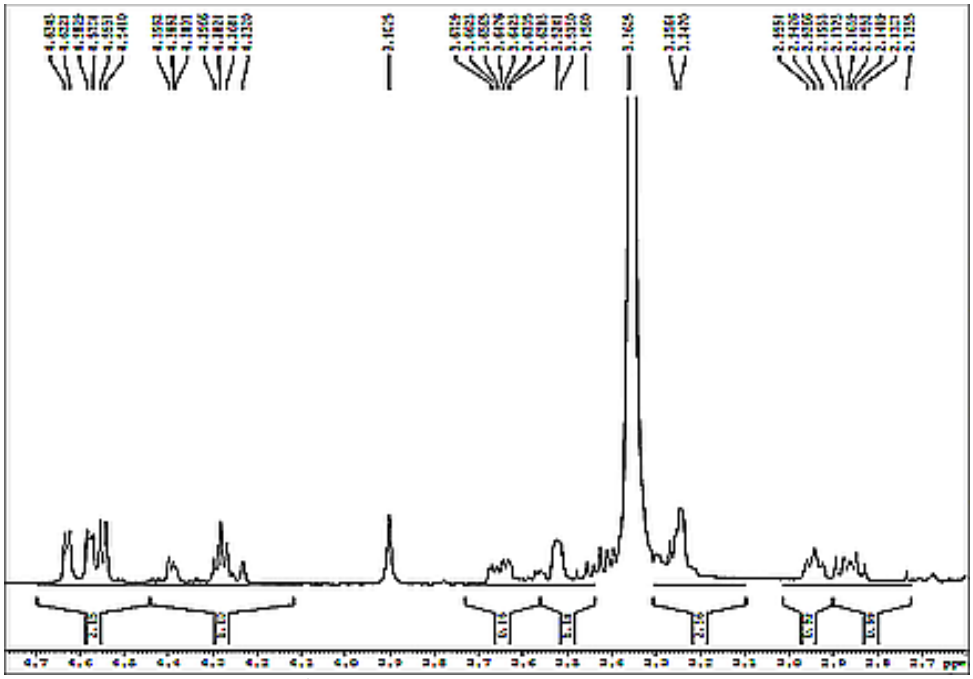

Figure2. [1]H NMR spectra of synthesized NODM.

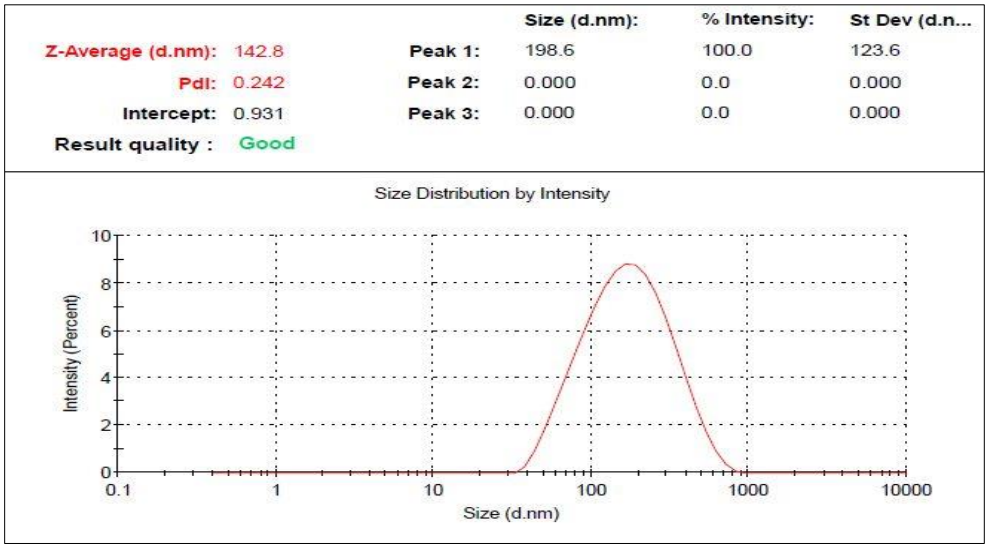

Figure3. Intensity plot showing particle size distribution of conventional SM NLCs.

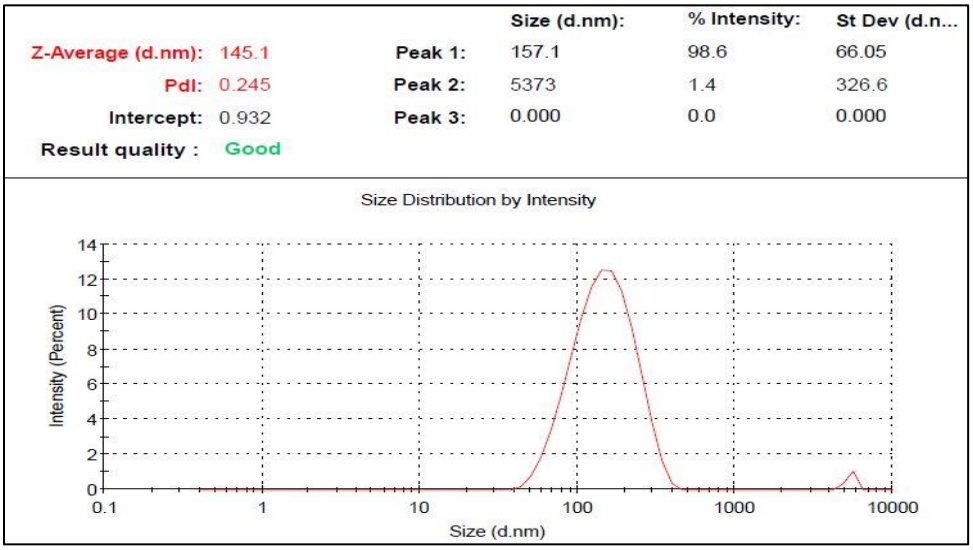

Figure 4. Intensity plot showing particle size distribution of mannosylated SM NLCs.

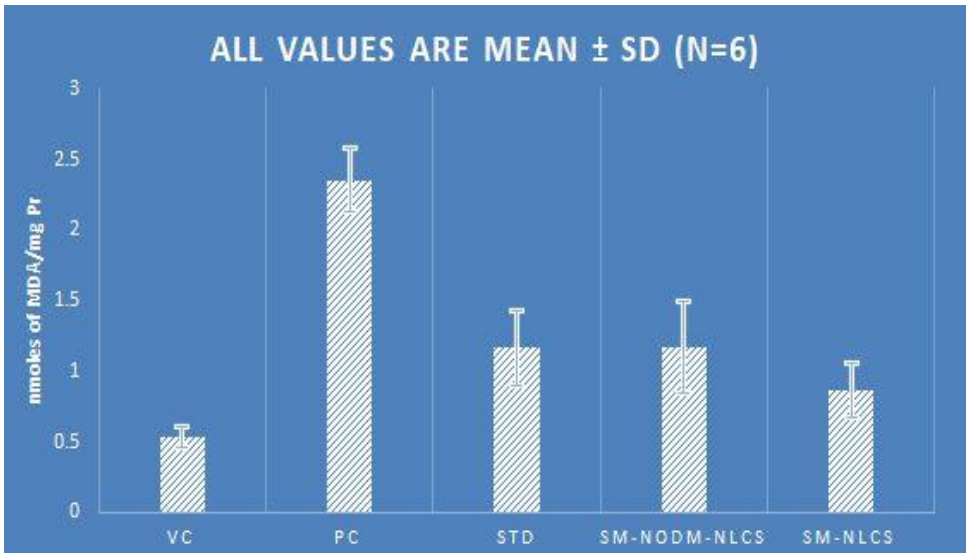

Figure 5. MDA levels on treatment with SM-NLCs, mannosylated SM NLCs and different control groups after CCl_4 induced hepatotoxicity.

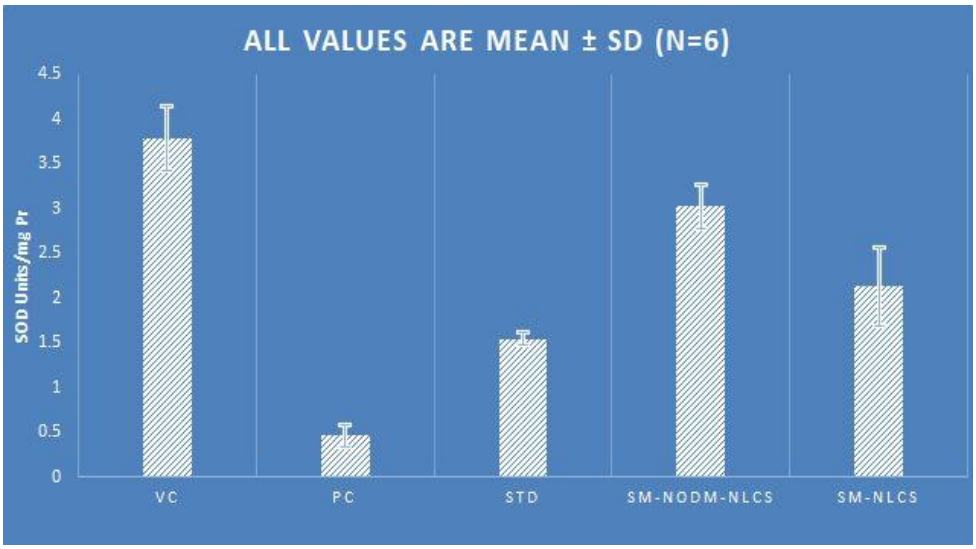

Figure 6. SOD levels on treatment with SM-NLCs, mannosylated SM NLCs and different control groups after CCl_4 induced hepatotoxicity.

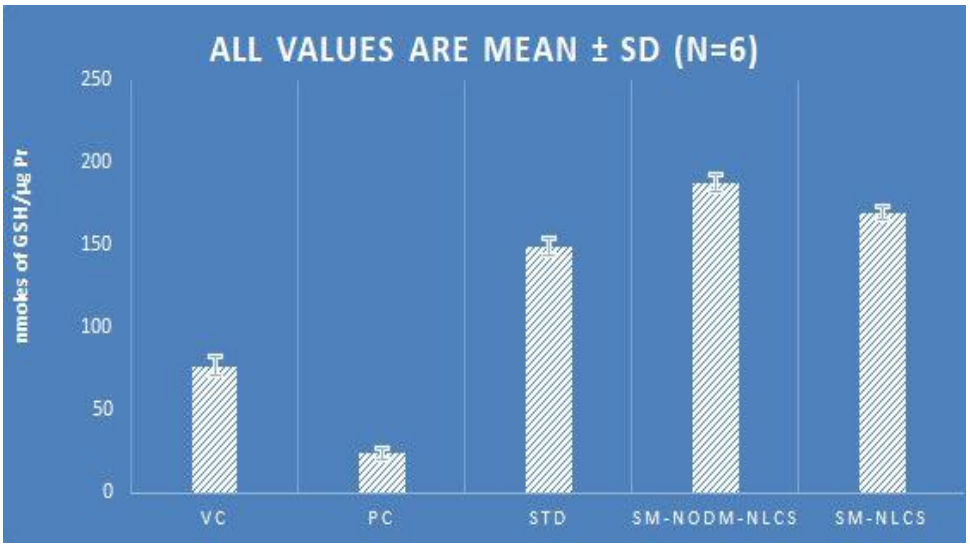

Figure 7. Chart showing comparative GSH levels on administration of SM-NLCs, mannosylated SM NLCs and different control groups after CCl_4 induced hepatotoxicity.

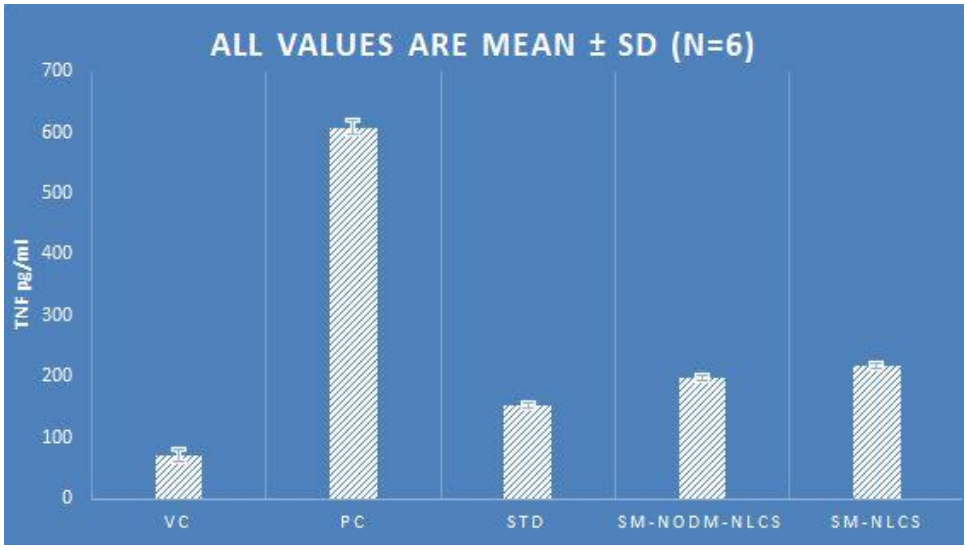

Figure 8. Comparative TNF-α levels on four weeks treatment with SM-NLCs, mannosylated SM NLCs and different control groups after CCl_4 induced hepatotoxicity.

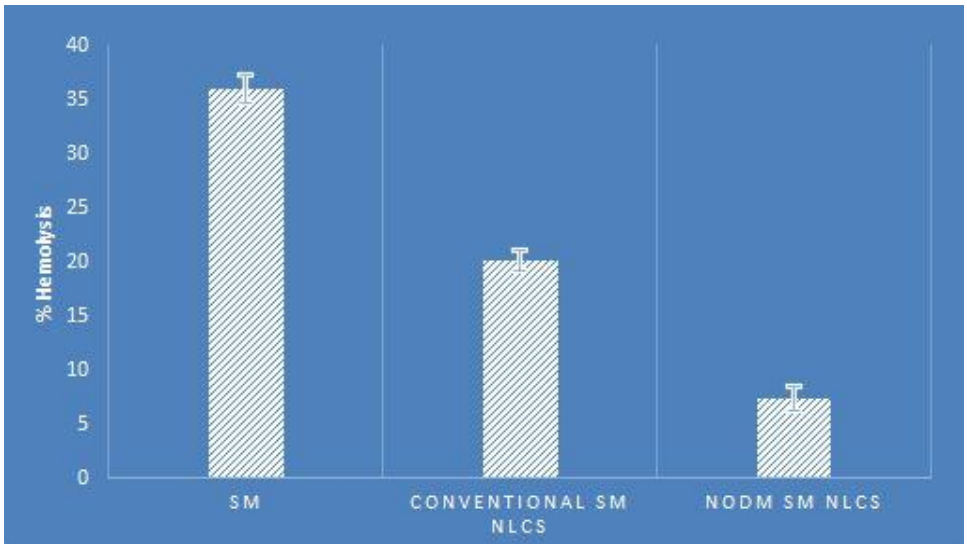

Figure9. Hemolytic toxicity study results showing % hemolysis due to free SM, conventional SM NLCs and mannosylated SM NLCs (n = 3).

Figure Legends

Figure 1.FTIR spectra of mannose, stearylamine and synthesized NODM.

Figure2.^{1}H NMR spectra of synthesized NODM.

Figure3. Intensity plot showing particle size distribution of conventional SM NLCs.

Figure 4. Intensity plot showing particle size distribution of mannosylated SM NLCs.

Figure 5.MDA levels on treatment with SM-NLCs, mannosylated SM NLCs and different control groups after CCl_4 induced hepatotoxicity.

Figure 6.SOD levels on treatment with SM-NLCs, mannosylated SM NLCs and different control groups after CCl_4 induced hepatotoxicity.

Figure 7. Chart showing comparative GSH levels on administration of SM-NLCs, mannosylated SM NLCs and different control groups after CCl_4 induced hepatotoxicity.

Figure 8. Comparative TNF-α levels on four weeks treatment with SM-NLCs, mannosylated SM NLCs and different control groups after CCl_4 induced hepatotoxicity.

Figure9. Hemolytic toxicity study results showing % hemolysis due to free SM, conventional SM NLCs and mannosylated SM NLCs (n = 3).